

Influence of Constant Current Accelerated Corrosion on the Bond Properties of Reinforced Concrete

Yang Sun¹, Guofu Qiao^{1,2*}

¹ School of Civil Engineering, Harbin Institute of Technology, Harbin, 150090, China

² Key Lab of Structures Dynamic Behavior and Control (Harbin Institute of Technology), Ministry of Education, Harbin, 150090, China

*E-mail: qgf_forever@hit.edu.cn qgfhit@163.com

Received: 9 January 2019 / Accepted: 5 March 2019 / Published: 10 April 2019

Reinforcement corrosion is one of the most serious durability problems faced by reinforced concrete (RC) structures. In the laboratory, current accelerated corrosion method is widely used to corrode RC structures. In order to reduce the experimental time, high current density always tends to be adopted in the experiments, but the effects of current on the mechanical properties of RC structures are neglected. In this study, four groups of RC members were corroded by current accelerated corrosion method, and the impressed constant current densities were $200\mu\text{A}/\text{cm}^2$, $400\mu\text{A}/\text{cm}^2$, $600\mu\text{A}/\text{cm}^2$ and $1000\mu\text{A}/\text{cm}^2$ respectively. The crack width of concrete and its corresponding power time were recorded in the accelerated corrosion process. After corrosion, the pull-out tests were performed to get the bond strengths of corroded RC members. The experimental results obtained indicate that increasing the magnitude of the impressed current density results in a significant increase in maximum crack width. In the attenuation model of bond strength, with the increase of impressed current, the critical corrosion level seems to decrease and the bond strength decreases sharply with the corrosion level.

Keywords: Corrosion; Current density; Crack width; Bond strength; Critical corrosion level

1. INTRODUCTION

Reinforced concrete (RC) is widely used as building materials in the world. One of the reasons why steel and concrete can work together is that good bond properties exist between these two materials. The bond properties are usually impaired due to corrosion of reinforcement when the RC structures serve in the harsh environment [1,2] such as stray current and coastal marine environment. In the process of reinforcement corrosion, the volume of oxidation might expand as much as six times [3]. These corrosion products accumulate on the steel/concrete interface (SCI), resulting in cracking of concrete cover and attenuation of bond strength. In order to study the effect of corrosion on the

structures and materials, many experimental methods have been adopted to corrode RC structures, like natural corrosion method [4], drying-wetting cyclic method [5,6], and current accelerated corrosion method [7,8]. Among these corrosion methods, current accelerated corrosion method is widely used, because it consumes less time to attain a relatively larger corrosion level. However, the effect of the impressed current magnitude on the mechanical properties of RC members are hardly taken into consideration.

Many studies [9–16] have revealed that the bond strength had an initial increase with slight corrosion reinforcement. This can be attributed to the increase of the interface roughness. When the steel bar continues to corrode, the bond strength will decrease rapidly induced by cracking of concrete cover. Moreover, the factors affecting the bond strength degradation are also studied. Experiments performed by Fang et al. and Lin et al. indicate that the stirrup can increase the bond strength to resist the effect of corrosion [9–11]. Tondolo et al. and Zhou et al. found that corrosion of the stirrups had a similar effect as the corrosion of the rebar on the bond strength degradation [12,13]. The experiments carried out by Wu et al. and Law et al. show that the thickness of the concrete cover and the diameter of the steel bar can also affect the bond strength [14,15]. In fact, the experiments carried out to investigate the degradation of the bond caused by reinforcement corrosion are very sufficient and detailed. However, in pursuit of less experimental time, many researchers chose higher current density in the process of current accelerated corrosion, totally ignoring that the current magnitude might have some impacts on the experimental results. The maximum current density adopted in the experiments by Al-Sulaimani even reached $2000\mu\text{A}/\text{cm}^2$ [16] which is thousands of times higher than that of natural corrosion.

In the process of reinforcement corrosion, cracking of concrete is also a noteworthy issue. Generally, the process of concrete cracking is divided into two stages [17,18]. (1) Corrosion products mitigate into the pores of the concrete along the steel/concrete interface [19]. Simultaneously, corrosion products accumulate on the steel/concrete interface, causing hoop stress in the concrete cover. When the stress reaches the tensile strength of concrete, cracking initiates. (2) Inner cracks extend to the surface of the concrete and the corrosion products start to mitigate to the corrosion-induced cracks [18]. The existence of cracks on the concrete surface actually provides a path of rapid ingress for the agent to severely attack the reinforcement, which will accelerate the corrosion process. Crack width on the concrete surface is usually regarded as a parameter to predict reinforcement corrosion [20–22]. Although some researchers chose to analyze the crack width from the natural corroded members in the experiments [20–22], many still tended to get the required data from the RC specimens corroded by accelerated corrosion method [23–26]. In addition, crack width can also be used to estimate bond properties. Lin et al. utilized the crack width to predict the bond degradation in corroded reinforced concrete, using impressed current density of $400\mu\text{A}/\text{cm}^2$ – $600\mu\text{A}/\text{cm}^2$ to accelerate corrosion [25]. It actually remains to be studied whether such impressed current magnitude will induce deviated results.

So far, a gap has still existed in knowledge concerning the effect of impressed current magnitude on the corrosion-induced crack propagation and bond degradation of RC members in the process of current accelerated corrosion. Thus, in this paper, four distinct magnitudes of constant current densities were adopted to accelerate corrosion of RC members, and then pull-out tests were performed on these corroded RC members to get the bond strengths. The effects of the impressed

current magnitude on the crack width and bond strengths were discussed and possible explanations were given.

2. EXPERIMENTAL PROCEDURE

2.1 Test specimen preparation

In the test, the central pull-out specimens were prepared without any stirrups configured in order to get the direct effect of the current densities. The cubic specimens were cast as the dimensions: 150mm × 150mm × 150mm. Each concrete cube was reinforced centrally with a HRB400 deformed steel bar with the length of 40mm and the diameter of 16mm. Before casting concrete, the actual length and the accurate mass of the steel bar were measured and were represented by l_0 and m_0 respectively. The thickness of concrete cover was 67mm, and the length of the bonded zone was 80mm, 5 times as long as the diameter of the steel bar. The unbonded length between concrete and steel was realized through a section of PVC tube with a length of 70mm, and the space between the PVC tube and the steel bar was filled with glass adhesives in case that the steel in the unbonded section corroded to influence the results. Fig. 1 shows the geometry and the dimension of the pull-out test specimens.

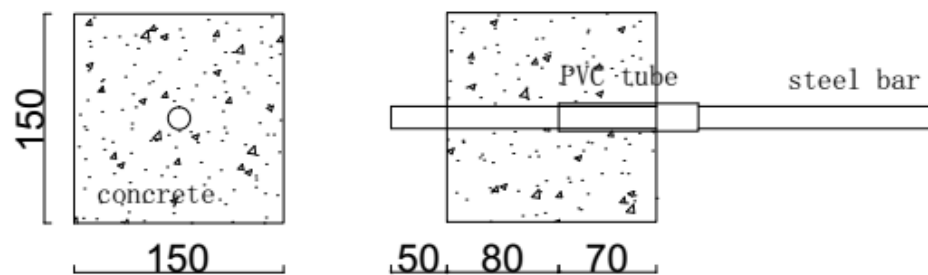


Figure 1. Geometry of the test specimens (all in mm).

The concrete was made with an ordinary Portland cement with the water/cement ratio of 0.314. The maximum aggregate size was 20mm. The concrete mix details are given in Table 1. The 28-day compressive strength of the concrete measured on 150mm × 150mm × 150mm cubes was in average 52.54Mpa. To keep the corrosion accelerated process in progress successfully, NaCl with a 5% mass ratio of Cl⁻ to cement was added to the mix.

Table 1. Mixture proportion of concrete (kg/m³).

cement	Fine aggregate	Coarse aggregate	Fly ash	Mineral Powder	water	Water reducing agent
400	716	1075	40	50	149	4.9

2.2 Current accelerated corrosion and crack observation

After 28 days of standard curing, all specimens were taken out from the concrete curing room.

The exposed sections of the steel, not in the concrete, were coated with a layer of epoxy resin. The junction of the steel and concrete was also protected to waterproof by the epoxy resin in case corrosion of reinforcement mainly concentrated here. After that, all specimens were soaked in a big plastic box filled with the NaCl solution with a mass ratio of 5% for 7 days before the accelerated corrosion process. The salt solution in the box was below the lowest point of the steel. Every other day, the specimens were turned around to keep every surface of the cubic wet.

With all specimens fully soaked, they were wrapped with a piece of wet sponge to maintain the moisture of the specimens, and on the outside of the sponge, a soft stainless steel net with many holes was used to wrap them. The current accelerated corrosion set-up is illustrated in Fig. 2. A controlled current source could apply a comparatively stable and adjustable impressed current. In the corrosion process, the steel bar served as anode, and the stainless steel net as cathode.

By reference to the current densities previously used by many researchers [16], four distinct magnitudes of current densities were chosen in the current accelerated corrosion method, namely $200\mu\text{A}/\text{cm}^2$, $400\mu\text{A}/\text{cm}^2$, $600\mu\text{A}/\text{cm}^2$, and $1000\mu\text{A}/\text{cm}^2$.

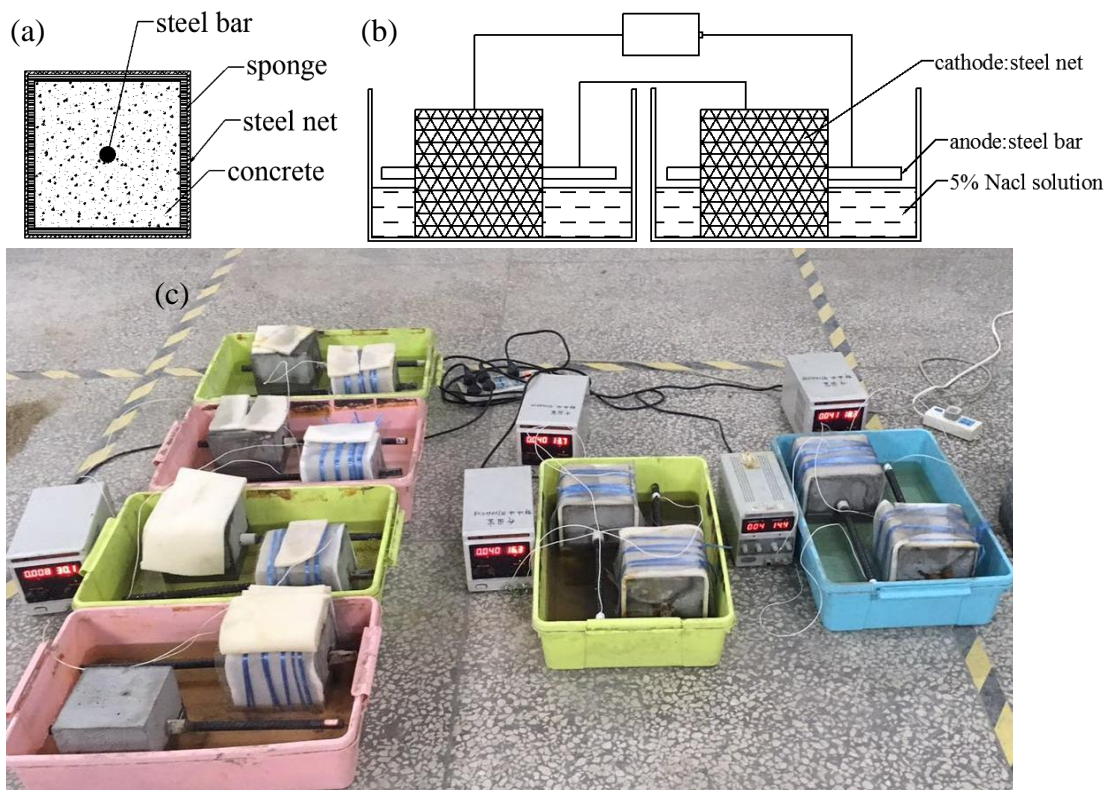


Figure 2. Scheme of the current accelerated corrosion set-up. (a) Wrapped-up concrete members. From inside to outside, it was steel, concrete, sponge and stainless-steel net respectively. (b) Circuit connection diagram. Reinforcement bar acts as anode and the stainless steel net as cathode. (c) Current accelerated corrosion of the RC members in the laboratory.

Two experimental groups were assembled. The first one comprised 4×6 specimens, and for every kind of current density, 6 specimens were prepared to corrode from 0 to 7%. In the process, these specimens were disconnected and extracted to measure and record the max crack width on the cross

surface of the concrete on different days. The second one comprised 4×9 specimens to perform pull-out tests after corrosion process. For every current density, 9 specimens were prepared to get their corroded bond strengths. Some of the specimens in the first group were used in the pull-out tests.

The theoretical corrosion time was calculated by Faraday's law which is expressed as below.

$$T = \frac{\Delta m \times Z \times F}{M \times I} \quad (1)$$

Where Δm is the mass loss of the steel in the bonded section (g); M is the atomic weight of iron (56 g/mol); I is the magnitude of the current (A); T is the power time (s); F is Faraday Constant, and its general value is 96500 A·s; Z represents the number of electrons lost in metal oxidation and it is generally considered that the atom of iron is oxidized to ferrous ion, which means that $Z=2$.

Considering the convenience of recording, the power time tends to choose the integer days which was slight longer than the calculated time instead of using the calculated time by Faraday's law directly. Generally, the higher the impressed current density, the more difficult it was to apply the current density. For the groups with the current density of 600 μ A/cm² and 1000 μ A/cm², 200 μ A/cm² was used to accelerate corrosion process in advance for about two days and then the corresponding current density was adopted in the experiments. During the process of the accelerated corrosion, much attention should be paid to the current magnitude in case it changed accidentally. If it changed a lot, some adjustments should be made to maintain the required current density.

2.3. Pull-out tests

When all members finished the process of current accelerated corrosion, they were taken out from the plastic box to perform the pull-out loading test on the MTS testing machine with the capacity of 300kN. Because the process of accelerated corrosion occurred in the steel and concrete interface, the effect of the current densities on the quality of steel/concrete interface was evaluated through pull-out tests. For the pull-out loading tests, the specimens were all loaded under displacement-control at a constant displacement rate of 0.5 mm/min. The loading procedures didn't stop until the bond failure occurred and the exerted load at this moment was automatically recorded by the MTS testing machine itself. The bond strength was calculated as follows:

$$\tau(\eta) = \frac{F}{\pi \times D \times L} \quad (2)$$

Where F is the maximum pull-out force recorded in the process of the test, namely the exerted force when the bond failure occurs; D is the diameter of the steel bar, and in this test $D=16$ mm; L is the length of the bonded section, and $L=80$ mm; $\tau(\eta)$ is the bond strength of the corroded RC members with corrosion level η .

After the pull-out loading procedures, the concrete around the corroded steel bar was broken up to extract the steel. Note that the mass m_0 and the length of each steel bar l_0 was measured before the experiments. The concrete residue on the steel was removed with a small brush, and the corrosion products of the corroded steel bar were cleaned according to the ASTM Standards [26]. The bonded zone of the steel with the concrete was cut off by a cutting machine, and the length l and weight m_0 were measured after this section was dried in the drying oven. The actual corrosion level η_A was

calculated by formula (3).

$$\eta_A = \frac{\frac{m_0}{l_0} - \frac{m}{l}}{\frac{m}{l}} \times 100\% \quad (3)$$

Where η_A is the actual corrosion level of the bonded zone; m_0 and m are the mass of the original steel bar and the cleaned corroded steel bar, respectively. Similarly, l_0 and l are the length of the original steel bar and the cut-off corroded steel bar of which the rusts have been removed, respectively.

Besides, the current efficiency ω was also calculated under different magnitudes of the current densities in the accelerated corrosion method, and it was the ratio of actual corrosion level η_A obtained by formula (3) to the theoretical corrosion level η_T calculated by Faraday's Law. The formula is as follows:

$$\omega = \frac{\eta_A}{\eta_T} \quad (4)$$

3. RESULTS AND DISCUSSION

3.1 Current efficiency in current accelerated corrosion method

The tests were intended to impress a constant current density, but in the early days of the experiments the current density gradually decreased. The reason for this phenomenon was that with the evaporation of water on the surface of concrete, the resistance of concrete increased gradually. Besides, the corrosion products entered the porous band in the steel/concrete interface in the electrochemical reaction. The corrosion accommodated region (CAR) became a dense layer and the transport of water and oxygen was limited [27], which led to a decrease in the current densities. This situation was the same as what Filipe Pedrosa et al. had observed [28]. However, several days later, the current density increased dramatically and crack appeared on the surface of concrete. The crack provided the access for the corrosion agents to inner concrete, so the RC members were easier to conduct electricity [27]. In the meanwhile, the corrosion products came out from the crack to the salt solution in the plastic box. In order to keep the current densities constant, the magnitudes of current were adjusted to the original values every six hours.

All the corroded steel bars were taken out from the concrete and cut off and cleaned to calculate the actual corrosion level η_A . The actual corrosion level was plotted against the power time under four different constant current densities in Fig. 3. As we can see from Fig. 3, for four groups of RC members with different current densities, the actual corrosion level η_A was approximately linear with time, with the difference of the specimen itself taken into consideration.

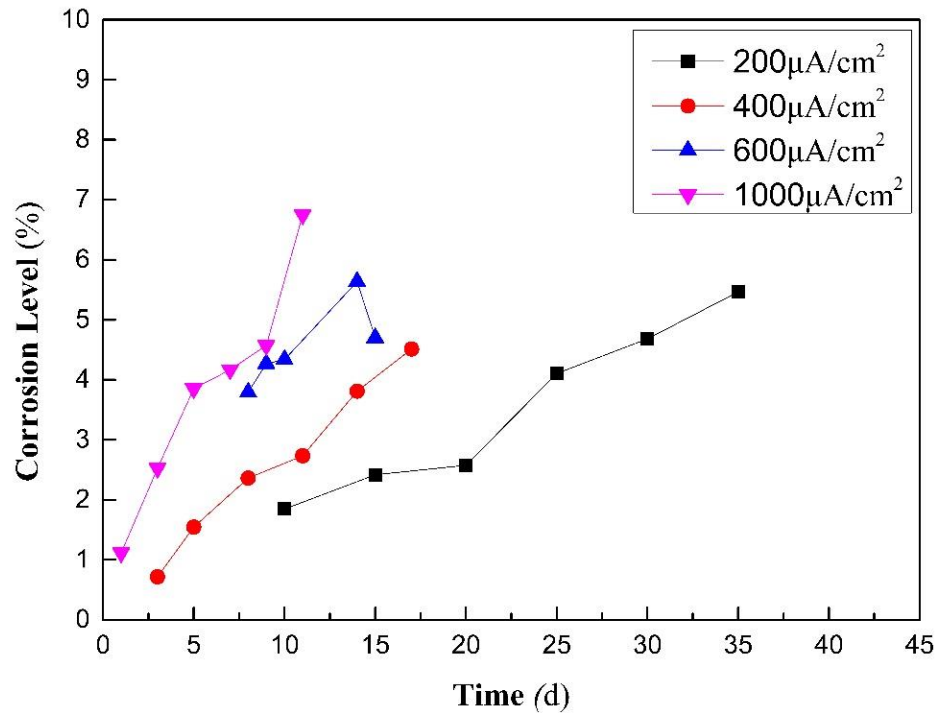


Figure 3. Actual corrosion level of corroded RC members

The actual corrosion level η_A of each specimen was compared with its theoretical corrosion level η_T , and the difference between them was reflected by current efficiency in this experiment considering the pre-accelerated corrosion. The current efficiencies were calculated and given in the Table 2, and we observed that the current efficiencies were not 100%, indicating that there existed a gap between the actual corrosion level and theoretical level, and the gap was significantly affected by the current magnitude. It was obvious that the current efficiencies of the specimens with $200\mu\text{A}/\text{cm}^2$ applied reached the highest, about 90% compared with that of $1000\mu\text{A}/\text{cm}^2$, 70%. Lower current density applied to the RC members induced higher current efficiency in the experiments. Note that the groups using $600\mu\text{A}/\text{cm}^2$ and $1000\mu\text{A}/\text{cm}^2$ adopted pre-accelerated corrosion which made the initial current efficiencies a little bit higher.

In the available literatures, some researchers believed that the totality of the impressed current was used to oxide the steel bar [28], and the current efficiency was considered to be 100% without any calculation. Nossoni et al. performed a series of experiments to investigate the effect of impressed current magnitude on the current efficiency ω in the accelerated method, and the results indicated that ω was generally less than 100% [29]. Similar results were obtained by Gustavo Duffó et al. [30]. The current efficiency lied between 1 and 45%. It is believed that competing reactions like splitting of water take place at the anode especially at low chloride concentrations and high current in accelerated corrosion testing of concrete [29,30]. Besides, when high chloride concentrates in the steel/concrete interface, chlorine gas might generate at the anode. Some chlorine gas corrodes the steel bar and some escapes from concrete cracks. This also can reduce the current efficiency. Another reason is the change of Z in the formula (1). Some iron atoms are directly oxidized to ferric iron ions rather than ferrous iron ions based on Pourbaix diagram. In calculating current efficiency, Z in the formula (1) should be 3 instead of 2 [8,29,30].

The current efficiency reported by Nossoni et al. reached 86% with the impressed current density of $700\mu\text{A}/\text{cm}^2$ and 3.5% NaCl solution [29]. It could be observed that in this experiment, the current efficiency was between 80%-60% with the current density of $600 - 1000\mu\text{A}/\text{cm}^2$, and it was close to the results obtained by Nossoni et al. [29]. In the experiments performed by Ballim et al. [31], the current efficiencies varied from 60% to 70% with the impressed current density of $400\mu\text{A}/\text{cm}^2$, which was similar to the values obtained in this experiment.

Table 2. Current efficiencies of every group with different current densities.

Current density	Current efficiency (%)					
$200\mu\text{A}/\text{cm}^2$	92.3	80.57	64.4	82.13	78.04	78.01
$400\mu\text{A}/\text{cm}^2$	71.69	84.36	80.56	67.74	74.25	72.38
$600\mu\text{A}/\text{cm}^2$	87.51	85.37	76.56	71.54	55.31	--
$1000\mu\text{A}/\text{cm}^2$	95.52	84.19	79.67	62.5	53.79	65.31

3.2 Crack on the surface of the concrete

The crack propagation on the cross surface of the concrete with time under different current densities were discussed in this section. We can see from Fig. 4 that the maximum crack width on the surface of the concrete increased linearly with time regardless of the magnitudes of the impressed current densities.

Meanwhile, in view of the different current densities applied in the experiments, total amount of electrical charge passing in the circuit was adopted to explore the relationship between the corrosion level and the maximum crack width. For the sake of simplification, the specific amount of electrical charge flowing in the circuit was replaced by the product of current density i and power time T , namely $i \times T$ [32]. As the Fig. 5 illustrated, with the same amount of electrical charge flowing in the circuit, the crack widths on the surface of the concrete were the smallest using the current density of $200\mu\text{A}/\text{cm}^2$, and it was apparent that for the specimens with the current density of $400\mu\text{A}/\text{cm}^2$ and $600\mu\text{A}/\text{cm}^2$, the crack widths were larger. This was caused by the fact that high current density led to large crack width even though the current efficiency dropped with increase of current density. When the current density reached $1000\mu\text{A}/\text{cm}^2$, the crack widths in the Fig. 5 dropped dramatically, but they were still larger than those with the current density of $200\mu\text{A}/\text{cm}^2$. The increased proportion of side effects in total reactions could account for this interesting phenomenon. The decrease of the crack width with the highest current density in this experiment was because of the decrease of the actual corrosion level of the steel bar compared with other specimens using lower current density, even though the high current density helped to increase the crack width. On the other hand, the corrosion products produced under the higher current density could hardly be fully oxidized in a shorter time [33].

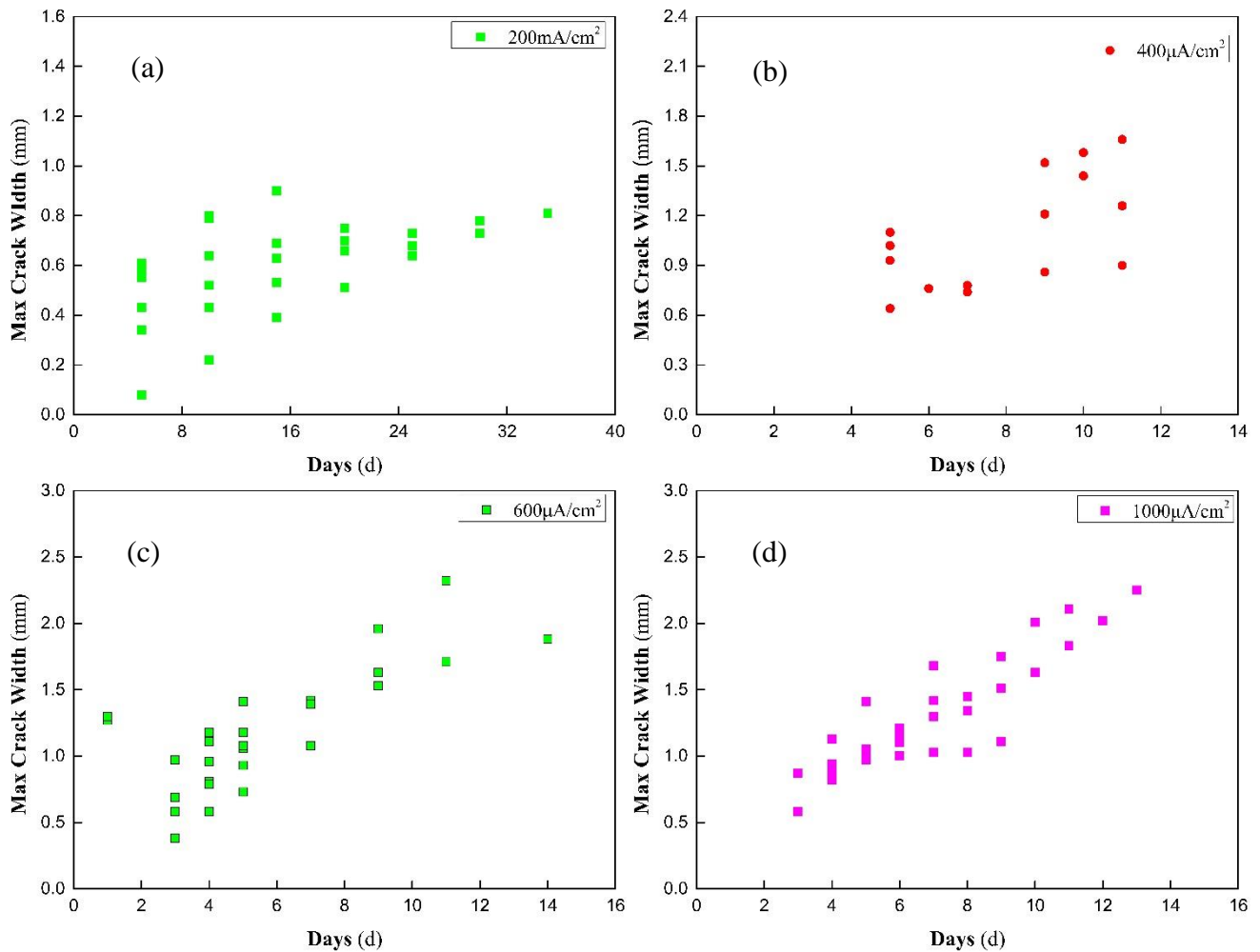


Figure 4. Evolution of max crack width with time under different current densities: (a)200 $\mu\text{A}/\text{cm}^2$, (b)400 $\mu\text{A}/\text{cm}^2$, (c)600 $\mu\text{A}/\text{cm}^2$ and (c)1000 $\mu\text{A}/\text{cm}^2$.

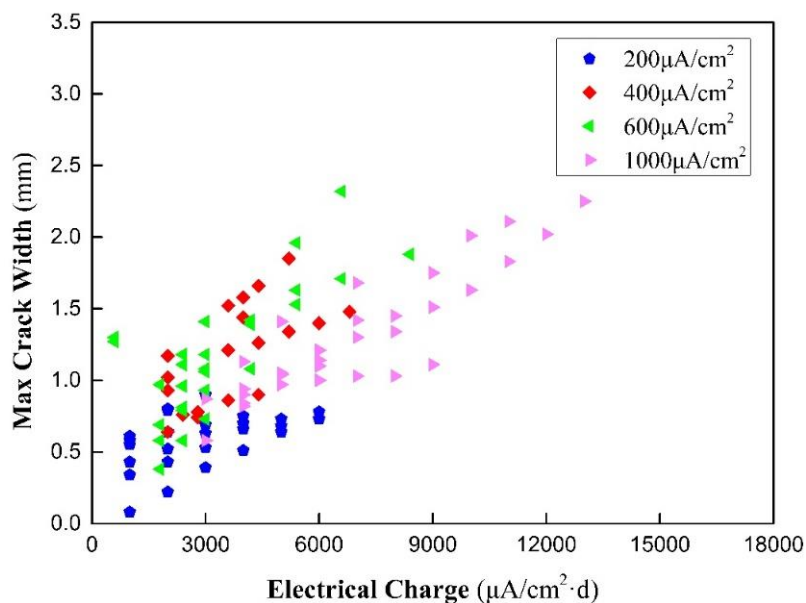


Figure 5. Evolution of max crack width with electrical charge flowing in the circuit, and the electrical charge($\mu\text{A}/\text{cm}^2 \cdot \text{d}$) = Impressed Current Density($\mu\text{A}/\text{cm}^2$) \times Power Time(d)

For the crack width, it can be perceived from the Fig. 6 that the high current density induced large crack width regardless of current efficiency in this paper. Maaddawy et al. [34] obtained the same conclusion using the actual corrosion level of the corroded steel bar even though the current efficiency exceeded 100%. Mangat et al. [35] also observed the similar phenomenon with the current density of 1, 2 and 3 mA/cm². On the other hand, Alonso et al. [36] revealed that the propagation of crack width was slower with a higher current density. The same conclusion was reached by Pedrosa et al. [28]. They suggested the slow and long-time corrosion loading would cause large deformation of concrete [28,36]. However, their adopted maximum current densities were relatively small (115 μA/cm² in [28] and 500 μA/cm² in [36]). To consider the effect of the current magnitude on the concrete, Mark G. Steward et al. [23] proposed a rate of loading correction factor K_R and believed that if the current density $i > 200\mu\text{A}/\text{cm}^2$, the cracking of concrete would propagate faster with a higher current density, which is basically consistent with the current range (200-1000μA/cm²) studied in this paper.

The development of corrosion layer (CL) can account for this phenomenon. Large amounts of corrosion products accumulate on the steel/concrete interface (SCI) with a high current density. When using a low current density, on the contrary, the corrosion products have enough time to mitigate into porous concrete (CAR) near SCI [23,34]. Current magnitude affects concrete cracking by the thickness of CL. CL of the specimens with a high current density is much thicker than that with a low current density. Large circumferential stress generates in the concrete layer with a high current density, causing the cracking of concrete. It is illustrated in the Fig. 6. The other reason is the localized stress concentration at the leading edge of the crack. After the inner crack reaches the surface of the concrete, corrosion products start to fill the crack [18]. With higher current density applied in the corrosion method, more corrosion products are produced in a less time and accumulate at the leading edge of the crack, and form localized stress concentration, leading cracks to widen. This is also observed by Dong et al. [37] using X-ray microcomputed tomography method. It is illustrated in the Fig. 7.

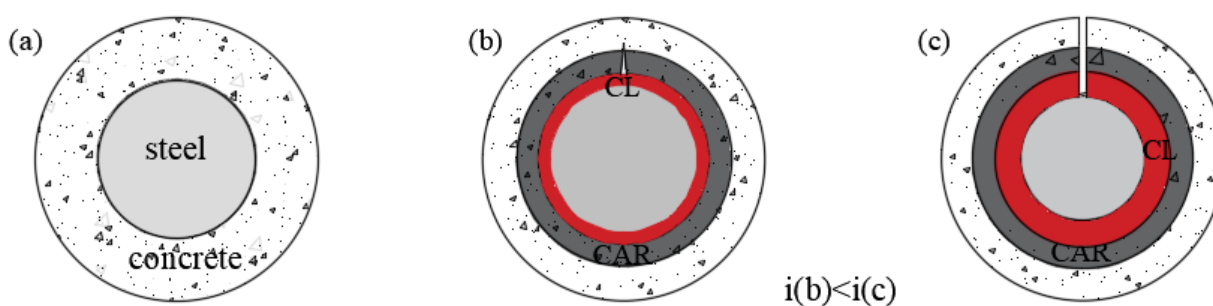


Figure 6. Diagram of corrosion development in the SCI. (a) no corrosion products produced. (b) Crack propagation induced by low current density (c) Crack propagation induced by high current density. The thickness of the CL: (a)<(b)<(c).

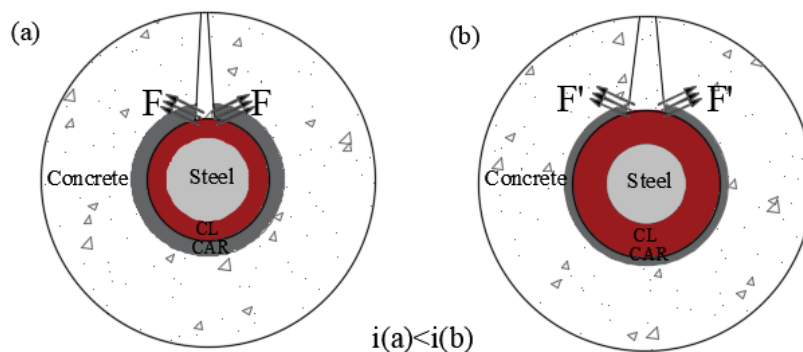


Figure 7. Diagram of crack propagation induced by localized stress concentration. The impressed current density: $i(a) < i(b)$. F and F' are induced by localized stress concentration, and $F < F'$.

3.3 Bond strength between the concrete and the corroded steel

The normalized bond strength $N(\eta)$ is usually used to evaluate the degradation of the bond strength when RC structures are under the influence of corrosion. The normalized bond strength represents the bond loss, which is the ratio of the bond strength after corrosion to that before corrosion. Its formula is as follows.

$$N(\eta) = \frac{\tau(\eta)}{\tau(0)} \tag{5}$$

Where $N(\eta)$ represents the normalized bond strength when corrosion level is η ; $\tau(\eta)$ is the bond strength when the corrosion level of the specimen is η ; $\tau(0)$ is the bond strength of non-corroded specimen.

The relationship between the normalized bond strength and the corrosion level has been investigated by many researchers [11,38–41]. Usually, the maximum corrosion level corresponding to the initial decrease of the bond strength is referred to as the critical corrosion level η_c . When the corrosion level η is less than the critical corrosion level η_c , the bond strength is regarded unchanged. However, further corrosion, which is larger than the critical corrosion level η_c caused a significant deterioration of the bond strength. Many researchers chose to fit the relationship between the normalized bond strength and the corrosion level by exponential form as listed in Table. 3.

Fig. 8 shows the normalized bond strength after corrosion with four different magnitudes of current densities. Whether using high or low current density, when the corrosion level was relatively low, the bond strength remained unchanged or floated up and down slightly. The low corrosion level would not severely damage the bond between the concrete and corroded steel. Meanwhile, it's noteworthy that the critical corrosion level η_c towards the degradation of the bond strength seemed to decrease with the increase of the current density. For the specimens with $200\mu A/cm^2$, the critical corrosion level η_c was between 1% and 1.5%. However, the critical corrosion levels η_c of the specimens with other three current densities were evidently below 1%.

Simultaneously, the current density used in the current accelerated corrosion method also played a part in degradation of the bond strength. The higher current density resulted in a lower bond strength. For example, when the corrosion level η was 2%-3% obtained by impressing $200\mu A/cm^2$ in

the experiments, the bond strength remained its 60% compared with 40% (400μA/cm²) and 10% (600μA/cm² and 1000μA/cm²). As shown in the Fig. 8, current magnitude had a direct impact on the decay of bond strength after corrosion, and with the increase of current density, the bond strength after corrosion decreased more sharply. The effect of the impressed current on bond strength degradation and change of critical corrosion level is illustrated in the Fig. 9.

There are two main reasons why the degradation of bond strength is affected by the current magnitude in accelerated corrosion method. One reason is that high current density will induce large crack width. The existence of crack on the concrete surface weakens the integrity of concrete, and consequently the protective effect of concrete cover is reduced. The crack width induced by corrosion is closely related to the bond strength [24,34]. With the same corrosion level, the larger the applied current density, the wider the crack width and the smaller the bond strength. Accordingly, the attenuation model of bond strength is affected by the current magnitude. Besides, as the first visible crack appears on the concrete surface, the corrosion level of steel bar is generally regarded as the critical corrosion level [38]. Large crack is produced with a high current density, and the critical corrosion level will be reduced. The other reason is that high current density can produce large amount of corrosion products in a short time, and most corrosion products accumulate on the steel/concrete interface, acting as a good lubricant. The bond strength between corroded concrete and steel decreases due to this lubrication. To get reliable and practical relationship between the bond strength and corrosion level, the effect of the current magnitude applied in the corrosion method cannot be ignored in the experiments, and more work still needs to be done to quantitatively analyze this effect.

Table 3. Attenuation model of bond strength with corrosion by previous researchers

Researchers	Relationships about the normalized bond strength	Notes
Lin et al. [11]	$N(\eta) = \begin{cases} 1 & \eta \leq 1.5\% \\ e^{-\delta(\eta-1.5\%)} & \eta > 1.5\% \end{cases}$	$\eta_c=1.5\%$; current density ranges from 400μA/cm ² -600μA/cm ²
Ma et al. [41]	$N(\eta) = \begin{cases} 1 & \eta \leq 2.41\% \\ 1.68\eta^{-0.59} & \eta > 2.41\% \end{cases}$	$\eta_c=2.41\%$
Chung et al. [40]	$\tau_{\max} = \begin{cases} 16.87 & \eta \leq 2.0 \\ 24.7\eta^{-0.55} & \eta > 2.0 \end{cases}$	$\eta_c=2\%$
Kapilesh et al. [39]	$R(\eta) = \begin{cases} 1.0 & \eta \leq 1.5\% \\ 1.192e^{-0.198\eta} & \eta > 1.5\% \end{cases}$	$\eta_c=1.5\%$; the formula is for the pull-out tests

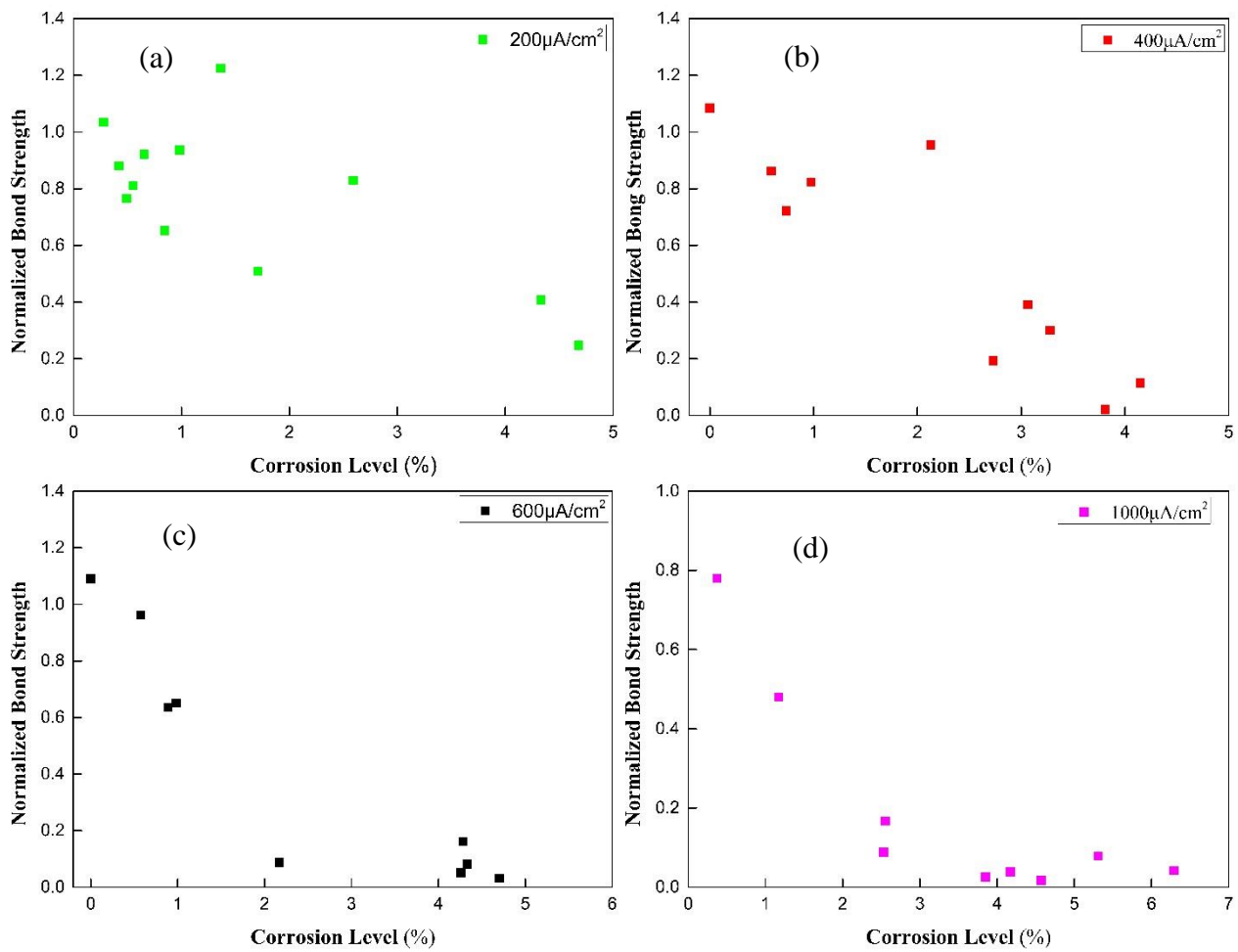


Figure 8. Relationships between normalized bond strength and corrosion level under different current densities:(a) $200\mu\text{A}/\text{cm}^2$, (b) $400\mu\text{A}/\text{cm}^2$, (c) $600\mu\text{A}/\text{cm}^2$ and (d) $1000\mu\text{A}/\text{cm}^2$.

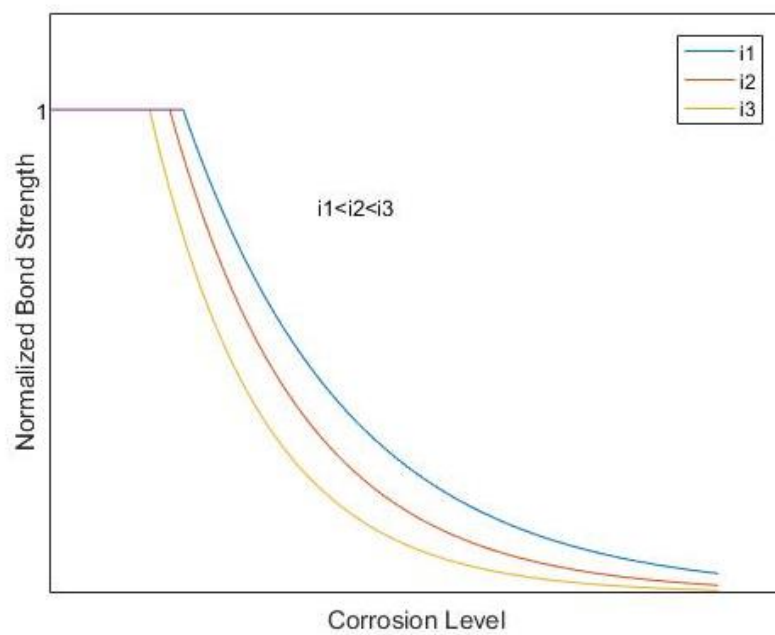


Figure 9. Diagram of the bond strength degradation affected by current densities

4. CONCLUSIONS

This paper deals with the crack width and bond strength of RC with different current magnitudes applied in the accelerated corrosion method. Based on the experimental results and discussions presented in the paper, the following conclusions can be drawn.

From the results of the corrosion, the current efficiency exists in the current accelerated corrosion of RC members, and the gap between the actual corrosion level obtained by weighing and the theoretical corrosion level calculated by Faraday's law increases with the increase of the current density. In the process of corrosion, the development of the maximum crack width on the concrete surface shows a liner relationship with time regardless of the current magnitude. However, high current density induces large crack width. Large amounts of corrosion products produce in the steel/concrete interface with high current density. These corrosion products have less time to mitigate into concrete, causing a larger hoop stress in the concrete. Meanwhile, accumulation of more corrosion products at the leading edge of the crack leads to localized stress concentration, which widens and propagates concrete cracking. The current magnitude further affects the attenuation of bond strength through development of cracks. The bond strength decreases sharply with a high current density. Simultaneously, the critical corrosion level gradually reduces with the increase of current magnitude.

ACKNOWLEDGEMENTS

The authors are grateful for the financial support of the National Key Research and Development Program of China (Projects No.: 2017YFC0703410, 2018YFC0705606), the Nature Science Foundation of China (NSFC) (Project No.: 51578190), the Special Fund for the Innovative Talents in the Field of Science and Technology in Harbin (Project No.: RC2014QN012014), the Fundamental Research Funds for the Central Universities (Project No.: HIT.BRET III.2012 33).

References

1. L. Bertolini, M. Carsana and P. Pedefferri, *Corros. Sci.*, 49 (2007) 1056.
2. M. Sosa, T. Pérez-López, J. Reyes, F. Corvo, R. Camacho-Chab, P. Quintana and D. Aguilar, *Int. J. Electrochem. Sci.*, 6 (2011) 6300.
3. S.J. Pantazopoulou and K.D. Papoulia, *J. Eng. Mech.*, 127 (2001) 342.
4. O. Poupard, V. L'hostis, S. Catinaud and I. Petre-Lazar, *Cem. Concr. Res.*, 36 (2006) 504.
5. T.A. Soylev and R. François, *Cem. Concr. Res.*, 33 (2003) 1407.
6. R.B. Polder and W.H.A. Peelen, *Cem. Concr. Compos.*, 24 (2002) 427.
7. J. Zuquan, G. Song, Z. Xia and Y. Li, *Int. J. Electrochem. Sci.*, 10 (2015) 625.
8. S.A. Austin, R. Lyons and M.J. Ing, *Corrosion.*, 60 (2004) 203.
9. C. Fang, K. Lundgren, L. Chen and C. Zhu, *Cem. Concr. Res.*, 34 (2004) 2159.
10. C. Fang, K. Lundgren, M. Plos and K. Gylltoft, *Cem. Concr. Res.*, 36 (2006) 1931.
11. H. Lin and Y. Zhao, *Constr. Build. Mater.*, 118 (2016) 127.
12. F. Tondolo, *Constr. Build. Mater.*, 93 (2015) 926.
13. H.J. Zhou, X.B. Liang, X.L. Zhang, J.L. Lu, F. Xing and L. Mei, *Constr. Build. Mater.*, 138 (2017) 56.
14. Y.Z. Wu, H.L. Lv, S.C. Zhou, and Z.N. Fang, *Constr. Build. Mater.*, 119 (2016) 89.

15. D.W. Law and T.C.K. Molyneaux, *Constr. Build. Mater.*, 155 (2017) 550.
16. G.J. Al-Sulaimani, M. Kaleemullah and I.A. Basunbul, *Struct. J.*, 87 (1990) 220.
17. Y. Zhao, Y. Wu and W. Jin, *Corros. Sci.*, 66 (2013) 160.
18. Y. Zhao, J. Yu, B. Hu and W. Jin, *Corros. Sci.*, 55 (2012) 385.
19. A. Michel, B.J. Pease, A. Peterova, M.R. Geiker, H. Stang and A.E.A. Thybo, *Cem. Concr. Compos.*, 47 (2014) 75.
20. T. Vidal, A. Castel and R. Francois, *Cem. Concr. Res.*, 34 (2004) 165.
21. I. Khan, R. François and A. Castel, *Cem. Concr. Res.*, 56 (2014) 84.
22. R. Zhang, A. Castel and R. François, *Cem. Concr. Res.*, 40 (2010) 415.
23. K. Vu, M.G. Stewart and J. Mullard, *ACI Struct. J.*, 102 (2005) 719.
24. S. Lim, M. Akiyama, D.M. Frangopol and H. Jiang, *Struct. Infrastruct. Eng.*, 13 (2017) 118.
25. H. Lin, Y. Zhao, J. Ožbolt and H.W. Reinhardt, *Eng. Struct.*, 152 (2017) 506.
26. G. Malumbela, M. Alexander and P. Moyo, *Cem. Concr. Res.*, 40 (2010) 1419.
27. Y. Yuan, Y. Ji and J. Jiang, *Mater. Struct.*, 42 (2009) 1443.
28. F. Pedrosa and C. Andrade, *Constr. Build. Mater.*, 133 (2017) 525.
29. G. Nossoni and R. Harichandran, *Corrosion.*, 68 (2012) 801.
30. G. Duffó, N. Gaillard, M. Mariscotti and M. Ruffolo, *Cem. Concr. Res.*, 74 (2015) 1.
31. Y. Ballim and J.C. Reid, *Cem. Concr. Compos.*, 25 (2003) 625.
32. S. Caré and A. Raharinaivo, *Cem. Concr. Res.*, 37 (2007) 1598.
33. W. Zhang, H. Zhang, X. Gu and W. Liu, *Constr. Build. Mater.*, 174 (2018) 675.
34. T.A. El Maaddawy and K.A. Soudki, *J. Mater. Civ. Eng.*, 15 (2003) 41.
35. P.S. Mangat and M.S. Elgarf, *Struct. J.*, 96 (1999) 149.
36. C. Alonso, C. Andrade, J. Rodriguez and J.M. Diez, *Mater. Struct.*, 31 (1998) 435.
37. B. Dong, G. Fang, Y. Liu, P. Dong, J. Zhang, F. Xing and S. Hong, *Cem. Concr. Res.*, 100 (2017) 311.
38. H.S. Lee, T. Noguchi and F. Tomosawa, *Cem. Concr. Res.*, 32 (2002) 1313.
39. K. Bhargava, A.K. Ghosh, Y. Mori and S. Ramanujam, *J. Struct. Eng.*, 134 (2008) 221.
40. L. Chung, J.H.J. Kim, S.T. Yi, *Cem. Concr. Compos.*, 30 (2008) 603.
41. Y. Ma, Z. Guo, L. Wang and J. Zhang, *Constr. Build. Mater.*, 152 (2017) 240.